CNRS
Centre National de la Recherche Scientifique

INFN
Istituto Nazionale di Fisica Nucleare

AdV - Stray Light Control: Baffling design around the cryogenic traps

VIR-0417B-13

A. Chiummo[1*], A. Moggi[2], and J. Marque[1,3]

[1] *EGO - European Gravitational Observatory*
[2] *INFN - Pisa*
[3] *J.Marque is now at Bertin Technologies*

Date: December 5, 2013

[*] *corresponding author:* antonino.chiummo@ego-gw.it

VIRGO* A joint CNRS-INFN Project - EGO* the European Gravitational Observatory
Via E. Amaldi, I-56021 S. Stefano a Macerata - Cascina (Pisa)
Secretariat: Telephone (39) 050 752 521 * FAX (39) 050 752 550 * Email: ego@ego-gw.it

Contents

Introduction

In the Advanced Virgo Interferometer (AdV), the contributions of technical noises are required to remain below the expected sensitivity (given by the fundamental noises) by a factor ten, that is to say the effective strain caused by technical noises must be $h_{tech}(f) < 1/10\ h_{AdV}(f)$ of the expected AdV strain sensitivity, over the whole detection bandwidth [1].
In order to fulfill safely this request, the SLC subsystem aims to set its own requirements for each single source of noise, within its scope, to be a further factor 10 below the safety margin. In other word, given the baffle $(Baf)_n$, contributing with a strain noise $h_n(f)$, SLC plans to achieve $h_n(f) < 1/100\ h_{AdV}(f)$, whenever possible and on "best-effort" basis. This should ensure that the overall noise contribution from items within the scope of SLC ($h_{SLC}(f)$) will be $h_{SLC}(f) < 1/10\ h_{AdV}(f)$.
In [2], requirements are derived for the optical characteristics of ground-connected surfaces, such as baffles, inside the Fabry-Perot resonators of AdV arms. These requirements allow to keep displacement noise not larger than the safety margin of ten, and translate into a maximum coupling efficiency for the scattered light to the main cavity mode of $|c^{(1/10)}_{xxBaf}|^2 = 10^{-24}\ W/W$. Appropriate scaling has to be applied to derive requirements that refer instead to the additional safety margin we want to impose.
Let us recall the equation for the strain noise induced by the baffle residual displacement [2]:

$$h_{Baf} = \frac{TF_{df/x_{Baf}}}{TF_{df/DARM}} \frac{1}{L_{arm}} |c_{xxBaf}| \times \tilde{x}_{Baf} \sim \frac{1}{L_{arm}} |c_{xxBaf}| \times \tilde{x}_{Baf}$$

where $|c_{xxBaf}|^2$ is the fraction of the power in the arm cavity that couples with the main mode after scattering from the baffle *xxBaf*. $TF_{df/x_{Baf}}$ is the transfer function from the baffle displacement noise to the dark fringe photodiode for a baffle that couples all the arm cavity power to the main mode, $TF_{df/DARM}$ is the transfer function from the differential-arm displacement to the dark-fringe photodiode, and $\tilde{x}_{Baf}$ is the displacement of the baffle if the amplitude motion of the baffle is small as compared to $\lambda/4\pi$ so that we are in the linear regime. When this condition does not hold true anymore, we are in regime of up-conversion of the motion. In this case a large low-frequency motion can give rise to strain noise at higher frequencies (phase wrapping). In order to perform the projection of the noise in this case, one has to replace the actual motion of the scatterer $\tilde{x}_{Baf}$ with an effective motion that gives the same power spectral density for the phase of the scattered field [3], namely: $\tilde{x}_{Baf}(\omega) = \frac{\lambda}{4\pi}\sqrt{PSD(\sin(\frac{4\pi}{\lambda}x_{Baf}(t))}$, where PSD indicates the power spectral density operator. From this equation, we can see that an additional safety margin of 10 means a factor $(1/10)^2$ for the coupling coefficient $|c_{xxBaf}|^2$, that becomes:

$$|c^{(1/100)}_{xxBaf}|^2 = 10^{-2}\ |c^{(1/10)}_{xxBaf}|^2 \sim 10^{-26}\ W/W \tag{0.1}$$

Starting from these requirements, we report here about the design of the baffles for the cryo-traps close to the towers housing the test masses, inside the arm cavities (see fig.1).

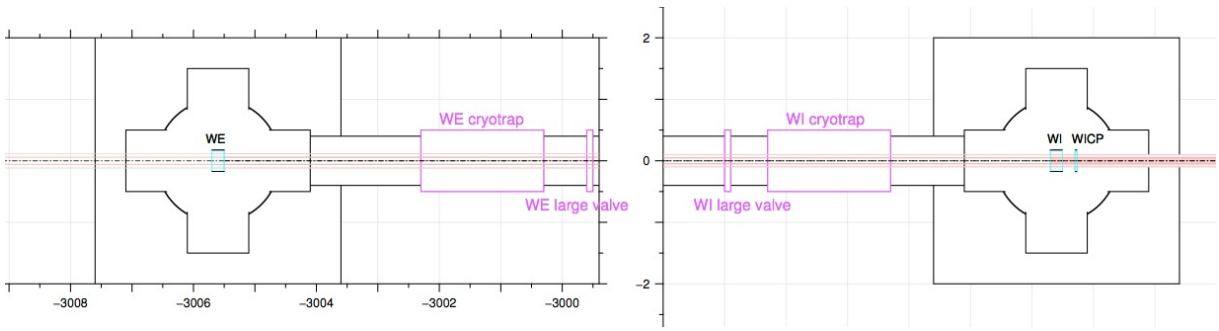

Figure 1: Sketch of the Advanced Virgo West Arm (not in scale). The large cryotraps between the test-mass towers and the long pipe will allow different vacuum levels in the two environments.

We will examine the case for the baffle at the entrance of the cryo-trap, tube-side (*Baf_Cryo*) and the one around the link inside the test-mass towers (*Baf_Tow*). We will refer to the two sides of each baffle as S_1, for the one facing the farthest test-mass mirror, and S_2, facing the closest test-mass mirror (see fig. 2).

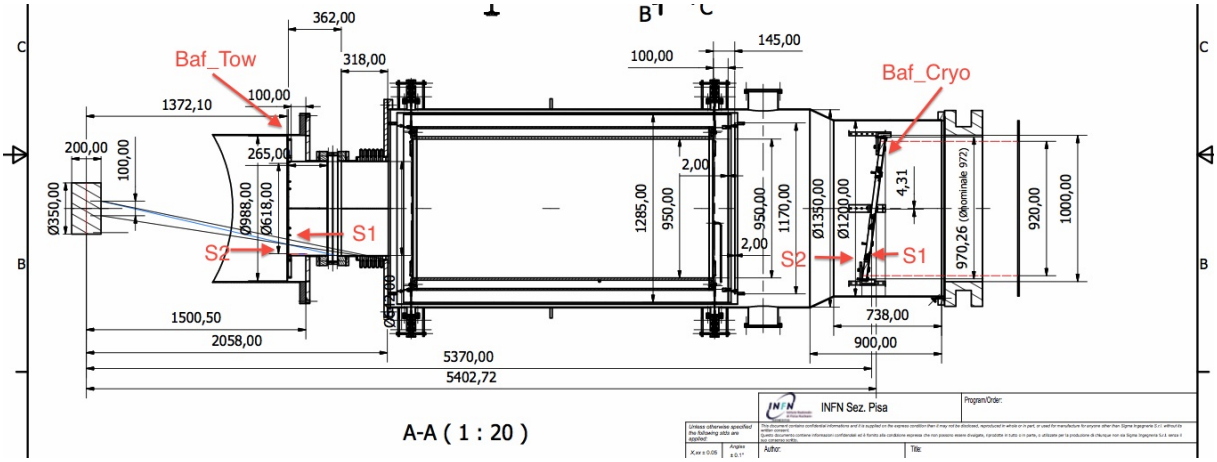

Figure 2: Mechanical layout of the WE Cryo-Trap, along with the Baf_Cryo and Baf_Tow where they should be installed (top-view). The final positions are still to be checked with the VAC subsystem, but from the first interactions we do not expect major changes. Surfaces of the baffles are referred to as S_1 for the one facing the farthest test-mass mirror, and S_2 for the opposite side.

1 Baf_Cryo

The baffle at the entrance of the cryo-trap (Baf_Cryo) must tackle part of the small-angle scattered light coming from the farthest test-mass (path-1: small-angle scattering, see [4]) and prevent the light from interacting with the cryogenic trap thermal baffles. Due to the wider angle, the side facing the closest test-mass is much less critical [2].

1.1 Material

The Baf_Cryo will be made of a plate of mirror-finish Stainless-Steel 304 ($TIS < 300ppm$, see [5]), with one side coated by a Diamond-Like Carbon layer to absorb the stray light impinging on it [5]. For the back-side, the one facing the closest test-mass, an oxidized plate of mirror-finish stainless-steel will be used.

1.2 Tilt angle

The tilt angle requirements for the Baf_Cryo are imposed by two considerations:

a) the tilt angle α must be such that the BRDF($\theta_s > \alpha$) of the surface side facing the farthest test mass (S_1) has already hit the minimum and is in the plateau regime. If we assume a BRDF law as it is for the test masses, then this occurs for $\alpha > 3°$;

b) the tilt angle must be such that the direct reflection off the surface $S2$ goes towards inner walls of the cryo-trap or the baffle around the closest test mass. This occurs for any ray coming from the beam-spot on the test-mass, when $\alpha > 5.5°$.

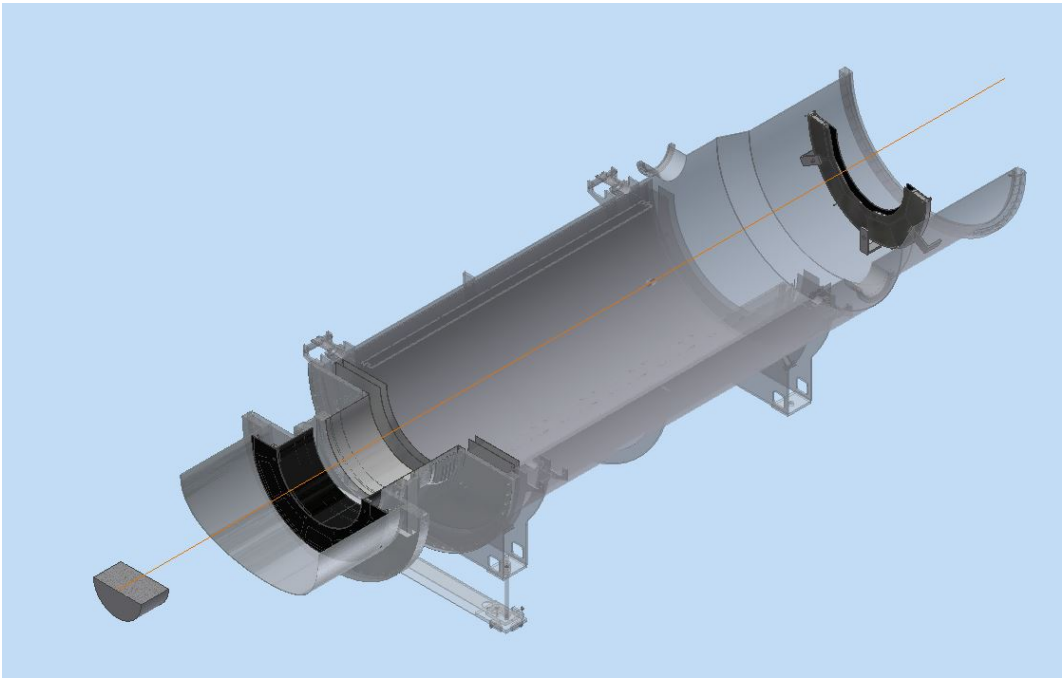

(a)

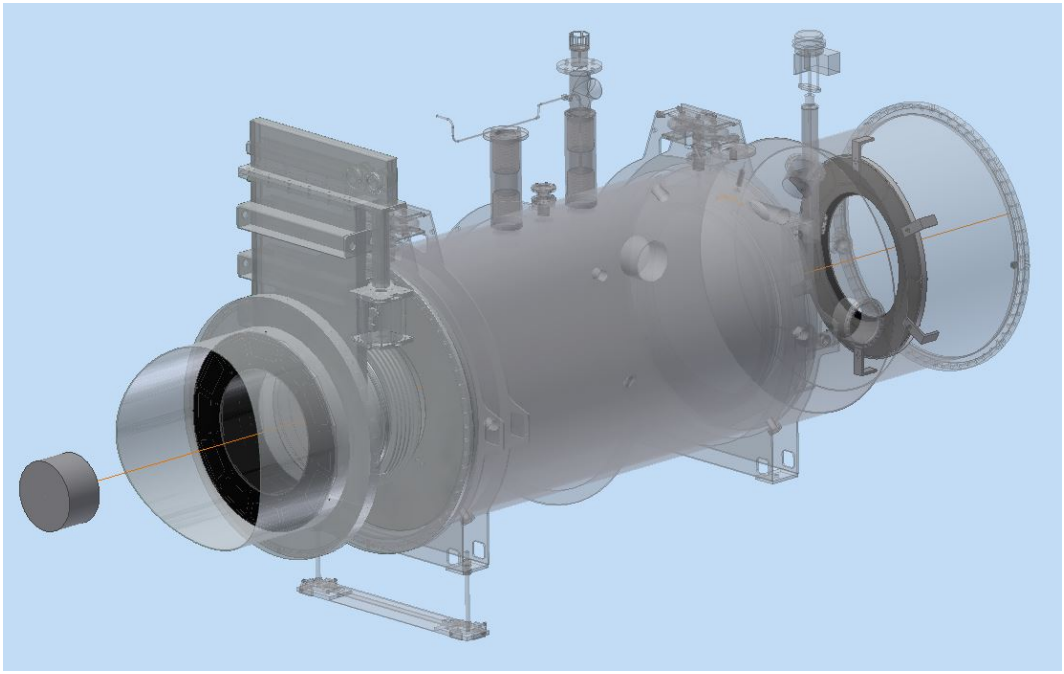

(b)

Figure 3: 3D mechanical layout of the Baf_Cryo and Baf_Tow where they should be installed - section view.

Therefore, by putting a) and b) together we decided:

$$\alpha_{Baf\_Cryo} = 7^\circ \tag{1.0}$$

There is no preferential axis of tilting from stray light considerations. Anyway, to ease the installation of possible wire-suspended baffles or the functioning of possible accelerometers on the back-side of the baffle, we chose the tilt around the y-axis. VAC had no objections to this choice.

1.3 Diameters

1.3.1 Outer diameter

Outer diameter $d^{out}_{Baf\_Cryo}$ must be as large as needed to overlap with the shadow cast by the closest baffle in the arm pipe, as seen from the farthest test-mass that sits some $3km$ away. According to [6], the diameter of this baffle is $d^{inn}_{PBaf} \sim 920mm$, and it is no farther than $l \sim 14m$ from the Baf_Cryo, so its shadow has almost the same inner diameter as the baffle in the pipe casting it. Taking into account the fact that the Baf_Cryo will be tilted around the y-axis (see sec.1.2), and hence the effective diameter will be shorter, we set $d^{out}_{Baf\_Cryo} = 940mm$ for the diameter of the coated area on the Baf_Cryo, so that:

$$d^{out}_{Baf\_Cryo} \cos(7^\circ) = 933mm > d^{inn}_{PBaf} \tag{1.0}$$

1.3.2 Inner diameter

Inner diameter $d^{inn}_{Baf\_Cryo}$ must be smaller than the aperture of the bottleneck between the tower flange and the pipe link, so to shade it from the farthest test-mass point of view. The bottleneck aperture is $650mm$ [1].

In order to find a lower limit for such a diameter, we carried out simulations with FOG [7]. These simulations aimed to find the coupling efficiency, $|c_{CBaf}|^2$, of the light scattered off the Baf_Cryo to the arm-cavity main mode, through the path-1, as a function of the inner aperture, and for different sets of maps describing the test masses. The outcomes of the simulations, reported in fig. 4, show that the coupling efficiency of the Baf_Cryo is well below the requirement $|c_{CBaf}|^2 < 10^{-24} W/W$ previously set in [2] (safety margin of 10), for clear apertures down to $d^{inn}_{Baf\_Cryo} > 550mm$.
From these results, we set:

$$d^{inn}_{Baf\_Cryo} = 600mm \tag{1.0}$$

Furthermore, we had recently the opportunity to access the actual measurements of the aLIGO test-mass figure error maps, courtesy of the LIGO Scientific Collaboration [8]. In [9] Marque et al. used those maps to perform the same simulations as we did for the expected (randomly generated) figure-error maps for AdV, in order to estimate the coupling of the scattered light to the cavity main mode. Despite the peculiar pattern of the coating on the aLIGO test masses, the outcome of the simulation was acceptable from the SLC point of view. With the aLIGO actual maps, and an inner diameter of $d^{inn}_{Baf\_Cryo} = 600mm$, the coupling efficiency was still $|c_{CBaf}|^2 \sim 4\ 10^{-25} W/W$.
All of the results for these simulations were obtained with a BRDF for path-1 of:

$$BRDF_{path(1)} = 3\ 10^{-3}\ sr^{-1} \tag{1.0}$$

For the case of this baffle, it would be rather demanding to achieve the safety margin of 100, so we must stick with the official safety margin of 10, that is anyway met with additional margin (a factor 2 or 3).

1.4 Inner edge

The baffle itself is tilted (about the y-axis) because of the considerations reported above. The inner edge angle must therefore comply with this tilt and cannot be cut at 90° with respect to the baffle surface, otherwise the

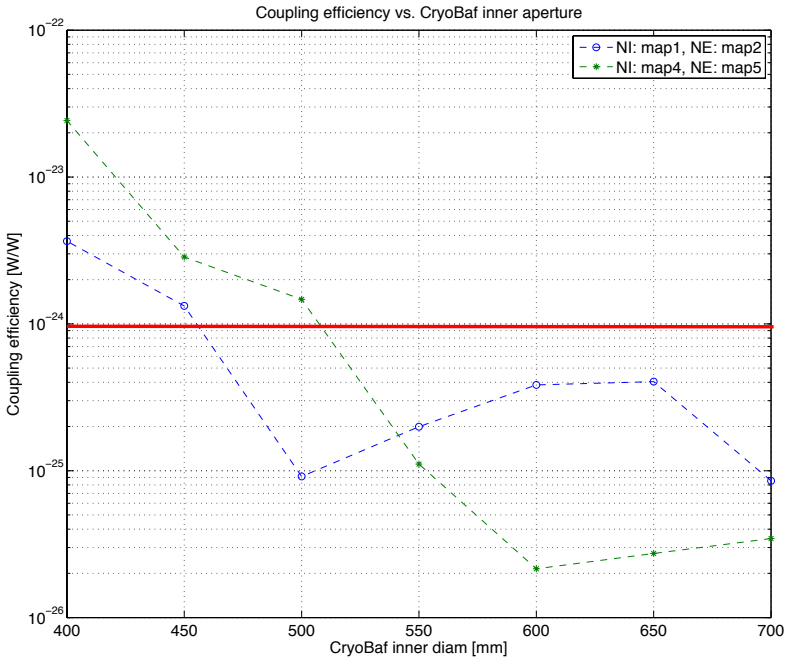

Figure 4: Coupling efficiency of light scattered off the Baf_Cryo versus its inner diameter. The red line marks the value $10^{-24} W/W$ that corresponds to the safety margin of 10. All of the results are obtained with $BRDF = 3\ 10^{-3}\ sr^{-1}$.

stray light coming from the test mass would see the uncoated reflective surface of the edge side. In order to avoid that condition, the edge angle will be $\alpha_{edge} \sim 80°$, so that $90° - 80° > 7°$.

1.5 Surface optical requirements

There are two surfaces of the Baf_Cryo that are important: the surface facing the farthest test mass, S_1, and the one facing the closest test mass, S_2. The requirements imposed on the optical characteristics of the two are quite different.
Indeed, while S_1 will be exposed to a power of the order of $\sim 2.5W$ when the ITF is locked at full power, S_2 will intercept a power $P_{CBaf_2} = P_{cav}\ BRDF_{Mir} \cos(\theta_{CBaf})\ \Omega_{CBaf} \sim 50mW$, almost two orders of magnitude smaller. Furthermore, while for S_1 the main path for coupling scattered light to the cavity mode is path-1, or small-angle scattering, the mechanism for S_2 involves wide-angle scattering from the test-masses (path-2).
In the following, we give specifications for both the surfaces.

1.5.1 Laser induced damage threshold

The expected maximum intensity on surface S_1 of the Baf_Cryo, for steady state operations and cavity power of $\sim 700kW$, is of the order of $\sim 2.5mW/cm^2$ [9], far from being a problem for most materials. When the arm cavity is not locked on resonance, then there is no power build-up, so the maximum intensity, I_{dir}, of the direct laser beam can be evaluated as:

$$I_{dir} = P_{in}\ T_{PR}\ \frac{1}{2}\ T_{IM}\ \frac{1}{\pi\ w^2} \sim 0.4mW/cm^2 \tag{1.0}$$

where standard values [1] have been used for the input power P_{in}, the power recycling mirror transmissivity T_{PR}, the input mirror transmissivity T_{IM}, and the beam size w.
As said, the surface side S_2 will intercept a power $P_{CBaf_2} \sim 50mW$ during steady state operations (locked arm cavity). So we do not need to worry about a laser induced damage for it.
Resuming, both the sides of the Baf_Cryo are not endangered by laser power and any material capable of enduring an intensity as low as $\sim 2.5mW/cm^2$ would be fine to build the surfaces.

1.5.2 Absorption

When the stray light impinges on the baffle surfaces, it is partly reflected off, partly scattered off and the remaining is refracted in the material of the surface. We require that less than 1000ppm of this refracted laser power manages to leave the baffles. In order to achieve that, surface S_1 will be coated with a $7\mu m$-thick DLC layer, capable of absorbing 99.9% of this refracted power on a round-trip (see [5]).
Surface S_2, on the contrary, will not be coated with any absorbing layer because the little power impinging on it that will mostly be reflected inside the cryo-trap vessel, thanks to the tilt angle.

1.5.3 BRDF

The Bidirectional Reflectance Distribution Function (BRDF) dictates the ratio of the impinging power that is scattered off a surface towards a given direction and within a given solid angle (see [10]). For surface S_1, the important path for the scattered light to couple back to the main cavity mode is what we termed path-1. The outcomes of the simulations we already reported in fig. 4 say that a $BRDF_{C1}(\theta_s > 7°) < 0.003sr^{-1}$ (eq. 1.3.2) is needed to fulfill the requirements of the strain noise induced by baffle expected displacement.
In order to achieve a negligible contribution for such a noise, we set:

$$BRDF_{C1}(\theta_s > 7°) < 3\ 10^{-3} sr^{-1} \tag{1.0}$$

This should allow to get $h_{CBaf_1}(f) < 1/30\ h_{AdV}(f)$.

The BRDF for surface S_2 is set starting from the requirements derived in [2] for path-2. By considering that the area of the baffle projected on a vertical plane is $A_{CBaf} = 0.46m^2$, and that the distance from the closest test mass mirror is $d_{CBaf} = 5.4m$, we can say that a $BRDF_{C2}(\theta_s > 7°) < 0.1sr^{-1}$ is enough to get $h_{CBaf_2}(f) < 1/100\ h_{AdV}(f)$.
Even a Lambertian scatterer with $TIS = 30\%$ would meet this requirement.

1.5.4 Reflectivity

Due to the tilt angle of the Baf_Cryo, the direct reflection from S_1 surface of the scattered light is prevented from reaching straightly the test masses. Nevertheless, the total power impinging onto this side of the Baf_Cryo is not negligible ($\sim 2.5W$ as said). The absorption coating on S_1 will be made of DLC, that presents a primary Fresnel's reflectivity, due to the refractive index, close to 15% at $\theta_{inc} = 0°$. So if left as it is, almost $0.5W$ would be free to wander in the arm pipes. In order to avoid that, we require the reflected power to be roughly of the same order of magnitude than the power scattered off from the baffle itself. Taking into account that a significant amount of power will be absorbed by the DLC coating, this leads us to require a reflectivity R_{C1} of the order of magnitude of the TIS for surface S_1. So we set:

$$R_{C1} < 0.5\% \tag{1.0}$$

Furthermore, from the calculations made in [2], we can see that the maximum area allowed for totally reflective surfaces at this distance from the closest test mass, and placed normally to an incoming ray, is of the order of $\sim 300cm^2$. This must be taken into account in the technical drawing when designing the mechanical mounts.

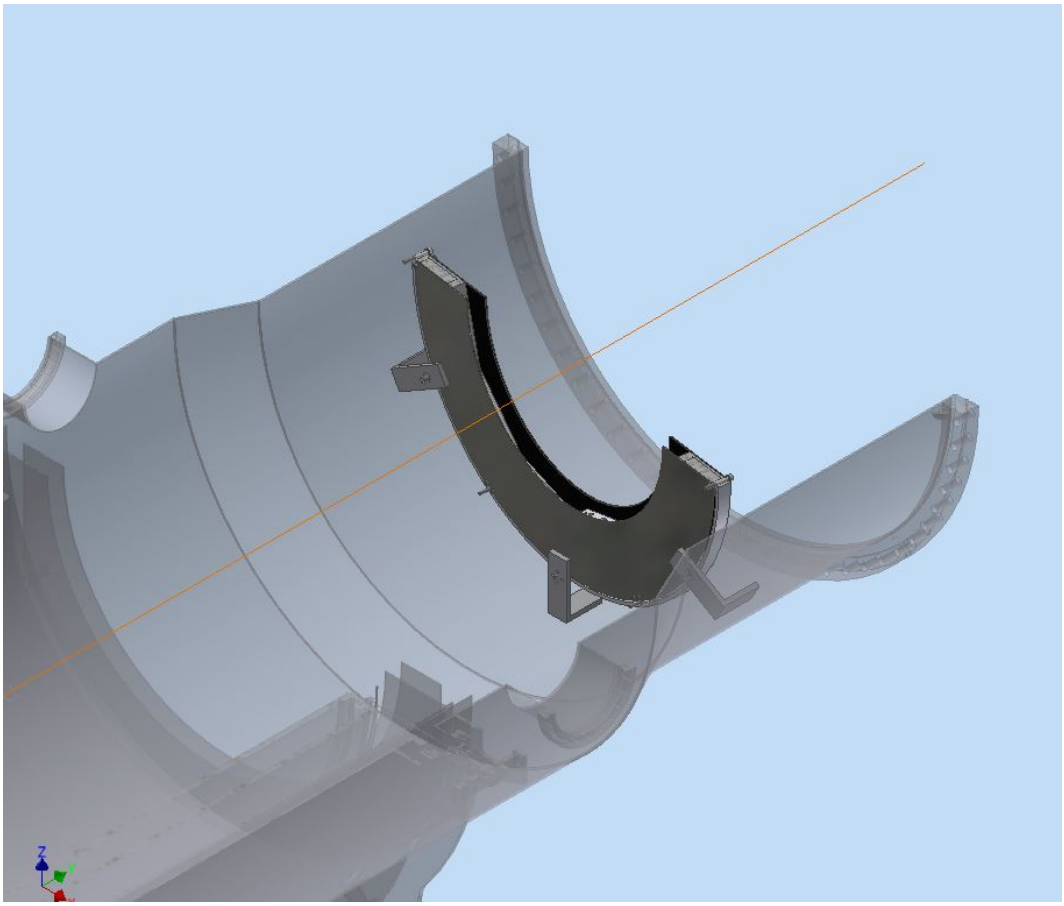

Figure 5: Close-up of a 3D section-view of the Baf_Cryo. The section in the picture shows the baffle with S2 surface facing the left of the picture.

1.6 Thermal requirements

Beside the obvious cooling effects, baffles and valves installed close to the cryotrap will be also heated, in vacuum, up to 120-150C during regenerations and bake-outs (order of a week per year). So the baffles and valves shall be designed to withstand this temperature range [11].
We performed a measurement of the temperature that a sample reaches when heated by a YAG laser beam, at intensity just below the laser induced damage threshold, and it was able to withstand $270°C$ without noticeable damage of the surface. This is in agreement with the vendor specs about this coating, stating that it can endure up to $400°C$ [12].

1.7 FEM mechanical simulation

The Finite Element Method used to predict the mechanical vibrations of the Baf_Cryo showed that the frequency of the first mode is rather low: $f_1 = 80.37Hz$ for the baffle alone. That is why we decided to attach the baffle to a frame with ribs, in order to push this lowest frequency as high as possible. In fig. 6 the first mode of vibration for the whole assembly baffle plus frame is depicted. This mode features a natural frequency $f_1 = 246Hz$.

2 Baf_Tow

The baffle around the bottleneck between the test-mass tower and the cryo-trap, namely the *Baf_Tow*, will sit on the tower side (see fig. 2), and will catch some of the wide-angle scattered light from the closest test-mass mirror through path-2. Its shape (see fig. 8 for a 3D view), is dictated by the need to hide the corrugated pipe inside the bottleneck without decreasing too much the clear aperture.

2.1 Material

The Baf_Tow will be made of a plate of mirror-finish Stainless-Steel 304, with one side coated by a Diamond-Like Carbon layer to absorb the stray light impinging on it, plus a further AR-coating to decrease the reflectivity to acceptable values.

2.2 Diameters

2.2.1 Outer diameter

In principle, the outer diameter of the Baf_Tow should be as large as possible to cover a solid angle as large as possible. In practice, there are several limitations due to the possibility to coat the surface, ease of handling/installing, and so on. The minimum value for the outer diameter must be such to cover the part of the flange of the tower that is exposed to the test-mass view. As a trade-off we set:

$$d^{out}_{Baf\_Tow} = 972mm \tag{2.0}$$

for the outer diameter of the coated area of the Baf_Tow. This will also ease the manufacturing process, as the external diameter is the same as the Baf_Cryo's.
Of course, this leaves a great extent of the tower walls exposed to the scattered light from the test-mass mirror it hosts. In order to tackle this stray light, the rest of the tower should be baffled with absorbing glass as in Virgo. This issue will be addressed in a future note.

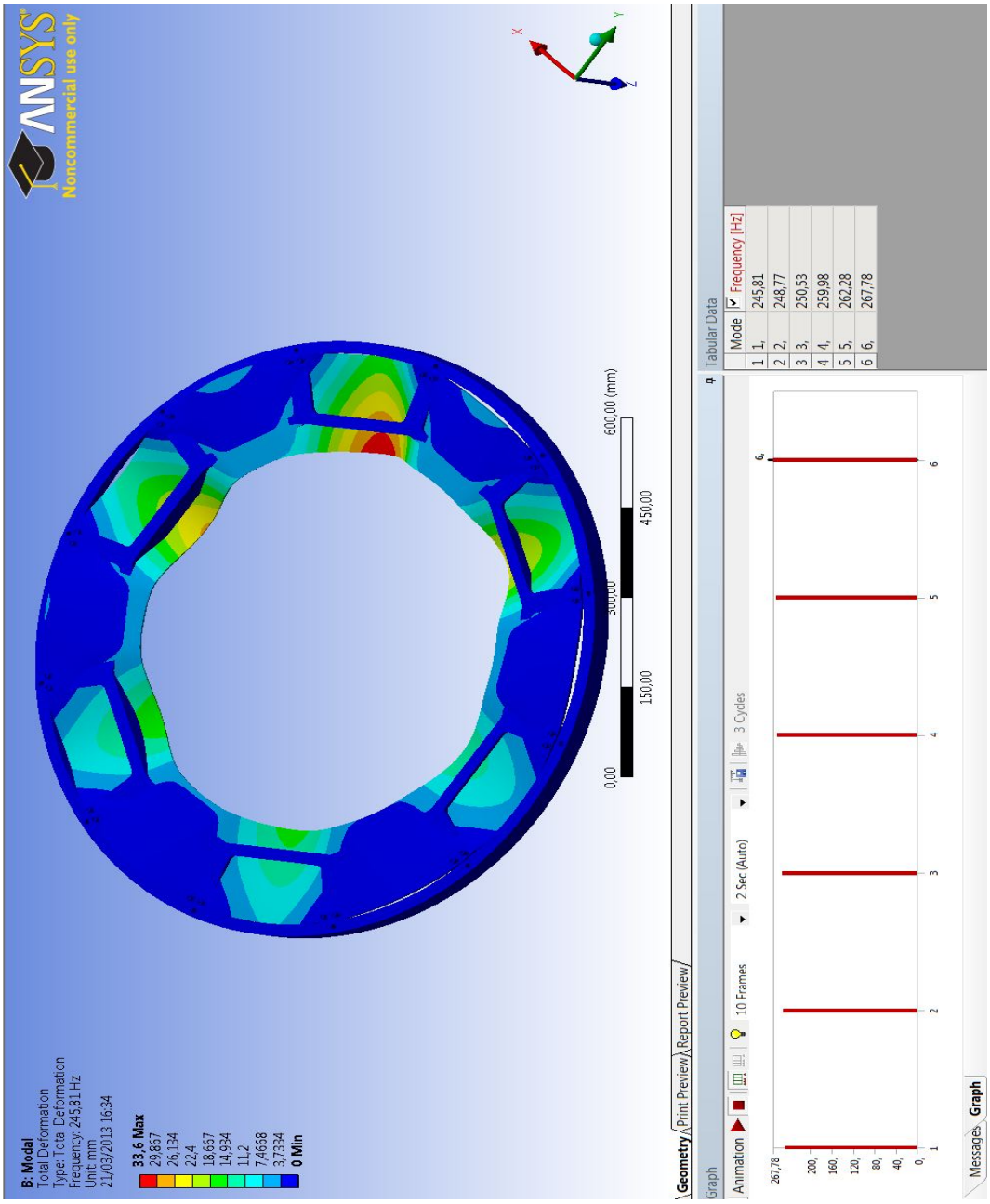

Figure 6: FEM simualtion for the whole assembly (baffle plus frame) of Baf_Cryo. The first vibration mode is depicted. This mode features a natural frequency $f_1 = 246Hz$.

2.2.2 Inner diameter

The inner diameter of the Baf_Tow should be not smaller than the clear aperture of the Baf_Cryo, so that its side S_1 is completely shadowed by the Baf_Cryo when seen from the farthest test-mass. Another problem is that the inner mountings and structures of the bottleneck between the tower and the cryo-trap would be exposed to the wide-angle scattering from the closest test-mass, if the inner diameter of the Baf_Tow cannot be shorter than the Baf_Cryo one (see fig. 7).

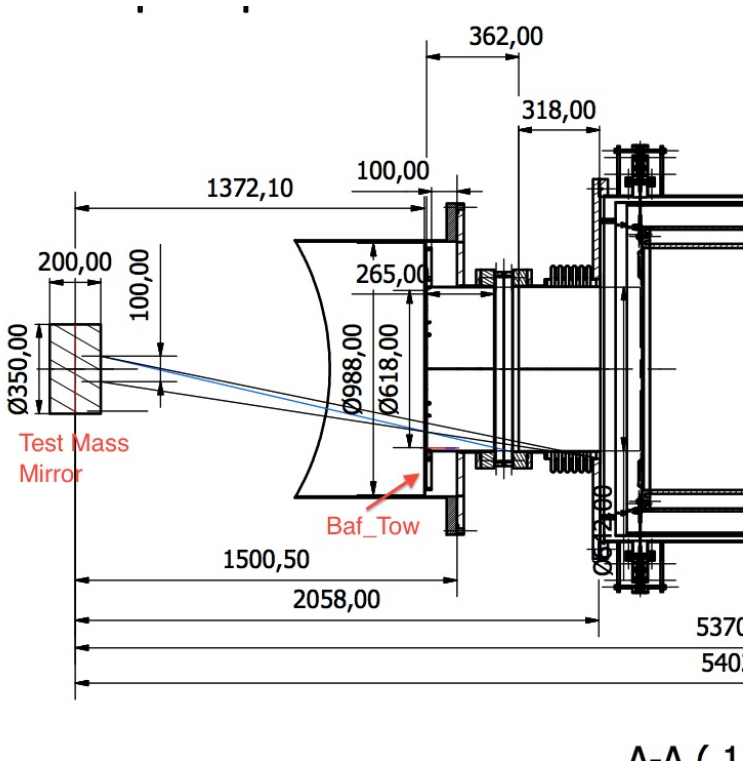

Figure 7: Close-up of a section-view of the Baf_Tow. The section in the picture shows the possible stray light from the test-mass mirror hitting the inner structures of the bottle-neck.

As a solution, we added a cylinder with rotation axis along the optical axis, so to cover the aforementioned structures.
From geometrical considerations, we set:

$$d^{inn}_{Baf\_Tow} = 618mm \tag{2.0}$$

for the inner diameter of the Baf_Tow. The added cylinder will have a slightly larger diameter, and height so large as to cover the inner structures of the bottleneck. The cylinder will be realized in two separate parts in order for the big valve to operate correctly (see fig. 8). The details of dimensions and sizes are being verified with VAC subsystem.
The cylinder will be realized in mirror-finish stainless-steel to ensure a low BRDF.

2.3 Tilt angle

The Baf_Tow will be perpendicular to the optical axis, so the tilt angle α with respect to the vertical will be zero:

$$\alpha = 0^\circ \tag{2.0}$$

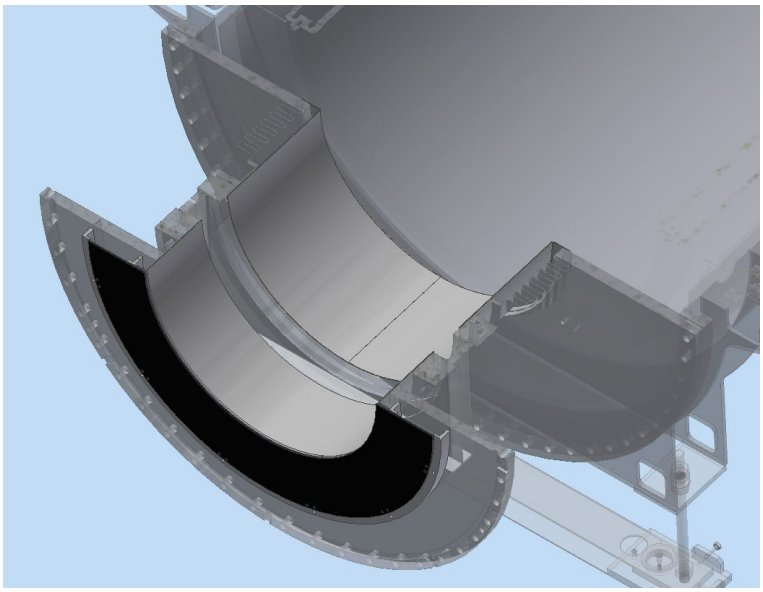

Figure 8: Close-up of a 3D-view of the Baf_Tow. The section in the picture shows the two-part horizontal cylinder needed to shield the inner structures of the bottle-neck. The separation between the two parts is needed to let the big valve be operated correctly.

Anyway, by taking into account the clear aperture, the minimum angle α_s for backscattering of the light coming from the closest test-mass will be:

$$\alpha_s = \arctan\left(\frac{d^{inn}_{Baf\_Tow}}{2\ dist_{Baf\_Tow}}\right) \sim 13^\circ \tag{2.0}$$

This angle ensures that the BRDF($\theta_s > \alpha_s$) has already hit the minimum and is in the plateau regime. This confirms also that there is no need for a further tilt of the baffle when the reflection is taken into account.

2.4 Inner edge

In order to avoid that the (usually rough and uncoated) side of the edge is seen from the test mass, we require an edge angle larger than 13° with respect to the optical axis. So we set $\alpha_{edge} = 70^\circ$ with respect to the surface of the baffle.

2.5 Surface optical requirements

There are three surfaces of the Baf_Tow that are important: the surface facing the farthest test mass, S_1, the one facing the closest test mass, S_2, and the inner surface of the horizontal cylinder S_{cyl}. The requirements imposed on the optical characteristics of these surfaces are quite different. Actually, while S_1 will not be seen at all from the test-masses point of view, S_2 will intercept a power $P_{TBaf_2} = P_{cav}\ BRDF_{Mir} \cos(\theta_{TBaf})\ \Omega_{TBaf} \sim 400mW$. Surface S_{cyl} will be seen from the test masses. The expected power impinging on such a surface will be $P_{TCyl} = P_{cav}\ BRDF_{Mir} \cos(\theta_{TCyl})\ \Omega_{TCyl} \sim 200mW$ from the closest test-mass, while the contribution from the farthest test-mass will be negligible, due to the very small solid angle of S_{cyl} as seen from 3km away ($\Omega_{Cyl} \sim 10^{-11} sr$).
In the following, we give specifications for all the surfaces.

2.5.1 Laser induced damage threshold

None of the surfaces of Baf_Tow is expected to handle dangerous intensities, so we are not concerned about this parameter.

2.5.2 Absorption

The only surface required to absorb power is the one facing the closest test mass mirror, S_2, that will therefore be coated with a $7\mu m$-thick layer of DLC. This will ensure that 99.9% of the power that manages to make its way through DLC will be absorbed.

2.5.3 BRDF

The surface S_1 will not be seen from the test masses, so we can neglect its contribution to the scattering.
S_2, on the contrary, will directly face the closest test mass mirror, and its scattering is susceptible of coupling to the main cavity mode through wide-angle scattering (path-2). The requirements for this surface can be derived from the calculations made in [2]. Baf_Tow is at a distance of $\sim 1.35m$ and the area of S_2 is $\sim 0.45m^2$, while the maximum allowed area for a $BRDF = 1$ is $\sim 0.04m^2$, ten times smaller. That means a maximum allowed $BRDF = 0.1sr^{-1}$ for wide angle scattering. If we want to impose a further safety margin as previously explained, we must set:

$$BRDF_{T2}\left(\theta_s > 13^\circ\right) < 10^{-3} sr^{-1} \tag{2.0}$$

The scattering from the surface of the horizontal cylinder, S_{cyl} could couple to the main cavity mode through the same mechanism of wide-angle scattering (path-2). At the distance from the test-mass where the Baf_Tow is, the maximum allowed scattering surface featuring a $BRDF = 1sr^{-1}$ is $area_{max} = 0.04m^2$ [2].
However, the requirements reported in [2] are referred to surfaces perpendicular to the axis linking the center of the test mass and the surface itself. If this is not the case, the surface has to be projected onto a plane perpendicular to said axis, so to subtend the same solid angle, and the BRDF adjusted for the cosine of the angle α_s between the normal to the scattering surface and the back-scattering direction (see fig. 5 in [2]). In other words, the requirements in [2] have to be regarded as for an effective BRDF, namely $BRDF^{eff} = BRDF/\cos\alpha_s$.
Let us denote with l the length of the cylinder, d the distance of the Baf_Tow from the test-mass surface, r_{inn} the inner radius of the Baf_Tow. The limiting angles for S_{cyl}, as seen from the center of the test-mass with respect to the optical axis, are:

$$\theta_1 = \arctan\left(r_{inn}/(d+l)\right) = 9^\circ \;;\quad \theta_2 = \arctan\left(r_{inn}/d\right) = 13^\circ \tag{2.0}$$

The area projected onto the plane perpendicular to said axis can be calculated as:

$$A_\perp = d^2\ \Omega_{Cyl} = d^2\ \pi\left(\cos\left(\theta_1\right)^2 - \cos\left(\theta_2\right)^2\right) = 0.14m^2 \tag{2.0}$$

The maximum allowed BRDF for the surface S_{cyl}, once projected and adjusted, is therefore:

$$BRDF_{Tcyl}\left(\theta_s > 9^\circ\right) < 10^{-2}\ \frac{area_{max}}{A_\perp}\ \frac{1}{\sin\left(\theta_2\right)} \sim 10^{-2}\ sr^{-1} \tag{2.0}$$

This value is already compliant with the stricter safety margin of 100.

2.5.4 Reflectivity

Surface S_1 cannot be seen from the test masses, so we are not concerned about its reflectivity.
Surface S_2 faces the closest test mass at a distance of $\sim 1.4m$, so the minimum angle of incidence for the light scattered off the test mass is $\alpha_i \sim 13^\circ$. This is enough to prevent direct reflection from hitting the test mass

mirror. Nevertheless, it is advisable to minimize the reflection due to the Fresnel's law, so to avoid some power bouncing on the tower walls. Surface S_2 will then be coated with AR film to have:

$$R_{T2} < 0.5\% \tag{2.0}$$

The reflection off surface S_{cyl} of the light scattered from the closest test mass will hit the cryo-trap walls and hence follow path-3 to couple with the arm cavity mode. But in [13] J-Y Vinet calculated as negligible such a contribution, so we will not be concerned about the reflectivity of S_{cyl}.
As for possible mechanical mounts on the S_2 side, the maximum allowed area for highly reflective surfaces at this distance from the test mass is $\sim 20cm^2$ *for the safety margin of 10*, while it becomes $\sim 0.2cm^2$ if we want to achieve the additional safety margin of 100. This means that there is *no room for reflective surfaces at all on* S_2 *side*. It is to be remarked that this statement refers to surfaces placed at 90° with respect to any beam coming from the test mass, so maximum care has to be payed in order to avoid such a situation.

3 Projection of baffle displacement noise to the strain sensitivity

The expected noise budget due to the residual displacement of the baffles around the cryotraps has been calculated as in [4] for the path-1 and [2] for the path-2. We computed the expected scattering of the major contributors for the West-End cryotrap, namely the surface (S1 cryo) facing the farthest test-mass and the one (S2 cryo) facing the closest test-mass of the Baf_Cryo, plus the surface (S2 tow) of the Baf_Tow facing the closest test-mass. This scattering was computed by supposing the BRDF set in the present note for each surface, and reminded in tab.1.
The overall noise due to the scattering off the baffles of the West-End cryotrap has been then obtained from the incoherent addition of noises computed for the single contributors. This is not strictly correct, since parts so close to each other are supposed to move coherently, but the phase relation between them is somewhat tricky (they can move with noise-cancelling phase) and a naive sum of the absolute values of the noises seems to be too pessimistic.
This exercise was done both for low μ-seism (50th percentile upper limit) and for high μ-seism (95th percentile upper limit), as communicated by Irene Fiori, see [4]. It is worth stressing that the seismic data are obtained by treating the whole modulus of the measured displacements as z-displacement, so their use is rather conservative.
The overall noise for the four cryotraps in the arm cavities has been computed by multiplying by a factor 2 the results from the West-End cryotrap (incoherent addition).
The results are reported in fig.9. It can be seen that the overall noise coming from the baffles of the four arm-cryotraps falls below the safety margin even for unusually high μ-seismic activity.

Table 1: BRDFs of baffles for cryotrap

Baffle surface	**BRDF** $[\mathbf{sr^{-1}}]$	**Coupl** $[\mathbf{W/W}]$
S2 Baf_Cryo	3×10^{-2}	$1.5\ 10^{-27}$
S1 Baf_Cryo	3×10^{-3}	$3\ 10^{-25}$
S_{Cyl}	$\sim 10^{-2}$	$\sim 10^{-26}$
S2 Baf_Tow	3×10^{-3}	$2.6\ 10^{-26}$

Conclusions

In this note we reported about the implementation in the baffle design of the specifications derived from the requirements computed in previous documents. In particular we reported about the baffle at the entrance of the Cryo-Trap (Baf_Cryo), and the one around the bottleneck between the test-mass tower and the Cryo-Trap (Baf_Tow).
All of the requirements translate into feasible implementations even considering a much tighter safety margin,

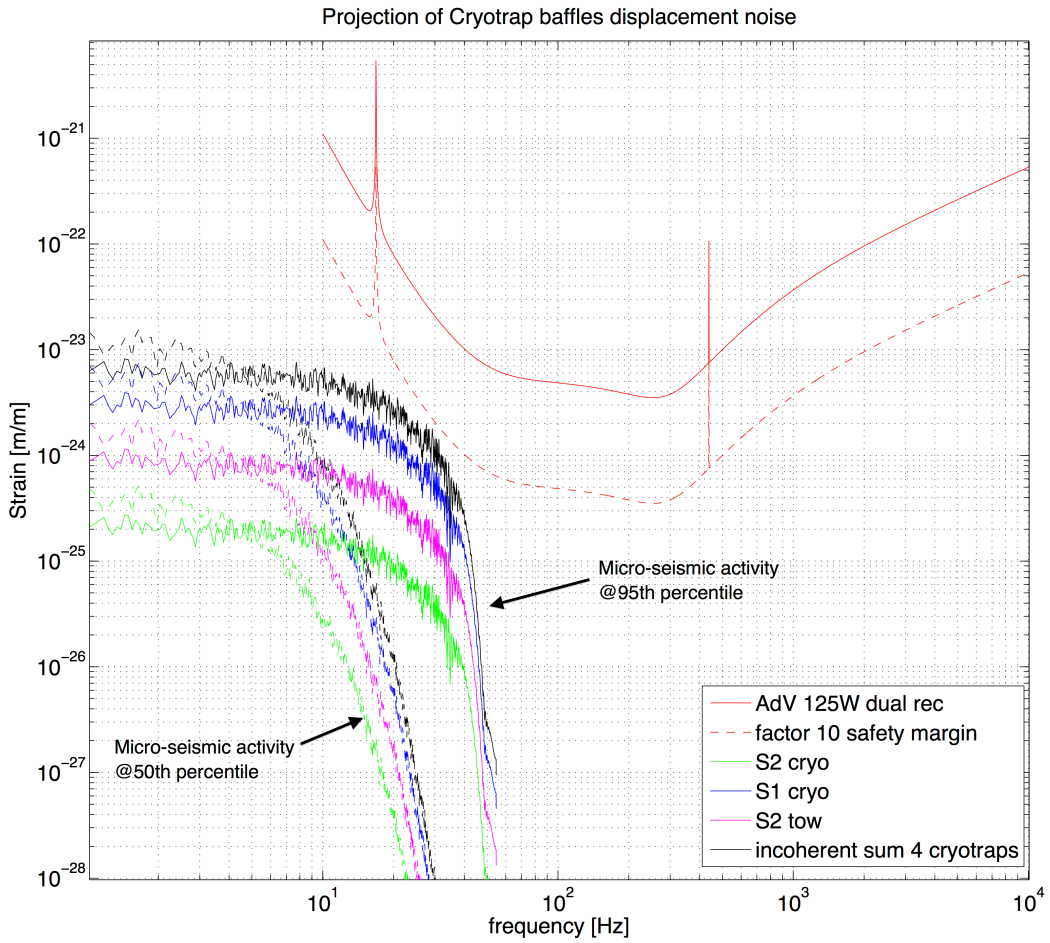

Figure 9: Noise projection of the displacement noise affecting the major contributors of the cryotrap baffles. The curves for the surfaces of Baf_Cryo and Baf_Tow are related to the West End cryotrap. The overall noise projection is estimated as the incoherent sum of the previously mentioned surfaces displacement noise times a factor 2 to account for the four cryotraps of the arm cavities. Solid lines are for high μ-seismic activity (95th percentile upper limit), dashed lines for usual μ-seismic activity (50th percentile upper limit).

100 instead of 10 times smaller than the predicted sensitivity, with the exception of the surface S_1 of the Baf_Cryo, where we expect to gain only a factor 3 or 4 with respect to the usual safety margin of ten. Anyway, when summing up all the noises coming from the scattering of all the relevant surfaces for the 4 arm-cryotrap, the result is still below the safety margin of ten. Therefore, no particular concerns arise from this exercise.
The only warning is about mechanical mounts close to the Baf_Tow, tower side. Due to requirements imposed upon high-reflective surfaces put at 90° with respect to the rays coming from the test-mass, *SLC advises strongly to avoid any exposed metallic surface around the Baf_Tow*. A possible solution could be the use of oxidized stainless-steel screws so tat their reflectivity is reduced. From the same requirements, an issue is identified for the tower walls that must be baffled to avoid direct scattering and/or reflection off them.
This issue will be addressed in a forthcoming note.

A Technical drawing of the Baf_Cryo

In figure 10, the technical drawing for the Baf_Cryo is reported. This design is frozen after interaction with VAC subsystem, the only pending issue being the details of the mountings. The Baf_Cryo is currently in production phase (substrates machined, ready to be coated).

Table 2: Features of BAF_CRYO

Baffle part	**materials**	**outer diam.**	**inner diam.**	**tilt angle**
S2 Baf_Cryo	Oxidized AISI304	972mm	640mm	7° (y-axis)
S1 Baf_Cryo	AISI304+DLC+AR	940mm	600mm	7° (y-axis)
frame	Alu 6061	984mm	726mm	7° (y-axis)

B Technical drawing of the Baf_Tow

The technical drawing for the Baf_Tow is still work in progress as of the writing of this version of the note. A preliminary drawing, without the cylindrical part, is in fig.12.

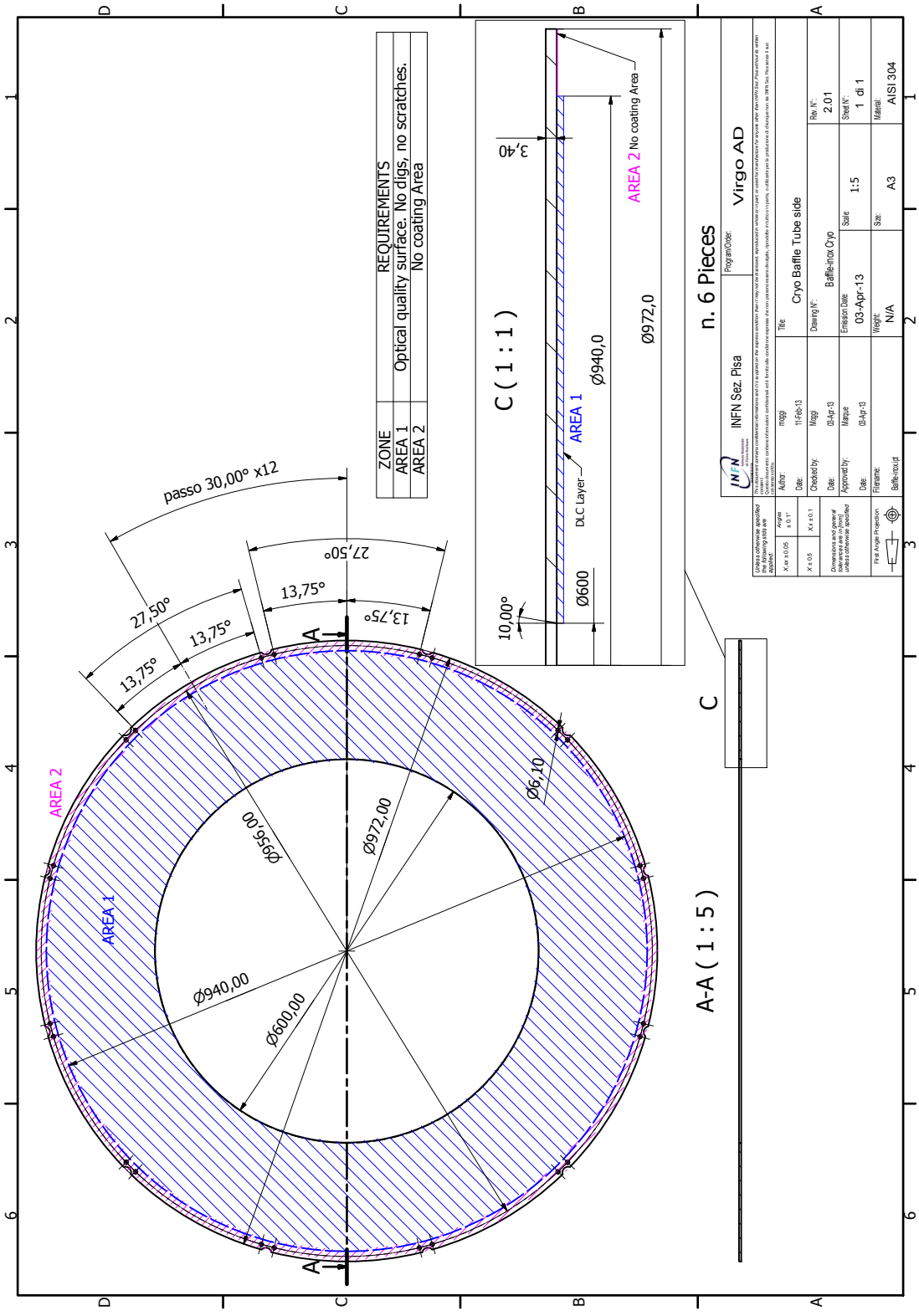

Figure 10: Technical drawing for the realization of the Baf_Cryo.

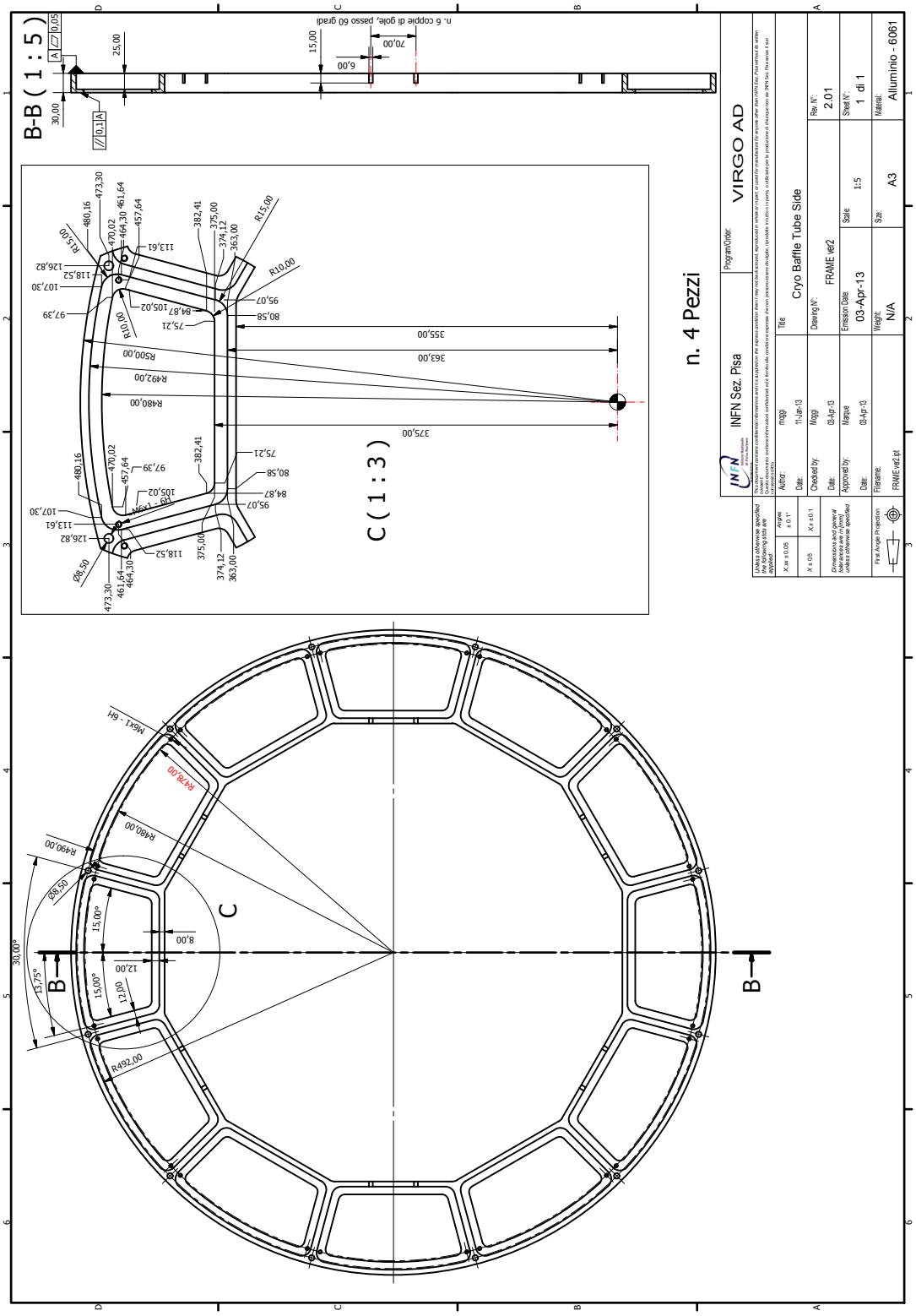

Figure 11: Technical drawing for the frame of the Baf_Cryo.

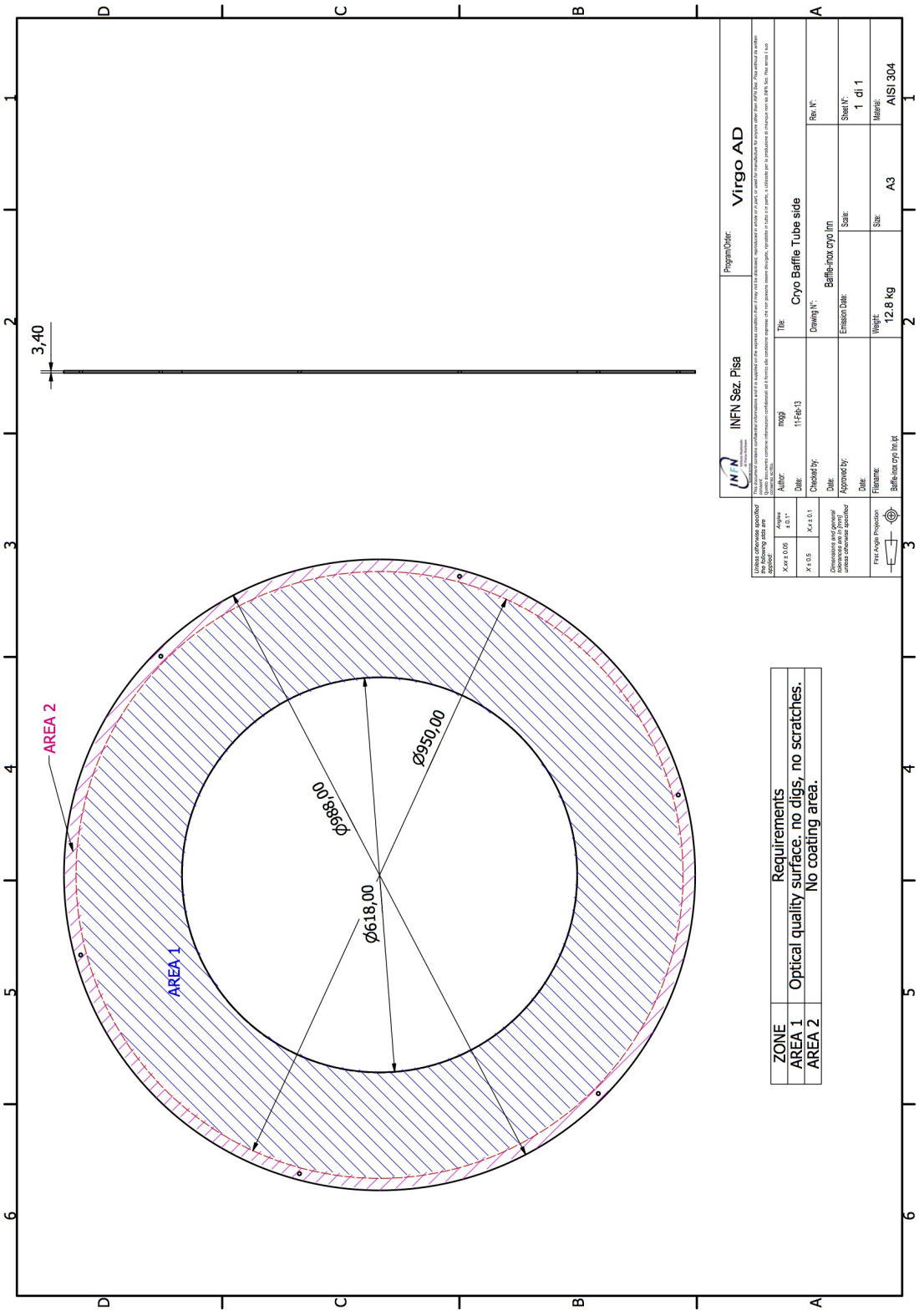

Figure 12: Draft of the technical drawing for the realization of the Baf_Tow.

References

[1] The Virgo collaboration, "Advanced Virgo Technical Design Report", VIR-0128A-12, and updates. 2, 5, 7

[2] A. Chiummo, R. Day, J. Marque, "Requirements for wide-angle scattering in the arm cavity", VIR-0055A-13 2, 3, 5, 7, 13, 14

[3] E. Flanagan and K. S. Thorne, LIGO-T940063-00-R 2

[4] A.Chiummo, J.Marque, "Calculation of displacement noise induced by the cryotrap baffle", VIR-0272A-12. 3, 14

[5] A. Chiummo, B. Canuel, A. Magazzu, and J. Marque, "AdV SLC: Characterization of Diamond-Like Carbon for coating baffles and beam dumps in AdV", Virgo technical note, VIR-0127A-13 https://tds.ego-gw.it/ql/?c=9472

[6] V.Brisson, personal communication to J.Marque.
T. Accadia, F. Acernese, M. Alshourbagy, et al. (The Virgo collaboration), "Virgo: a laser interferometer to detect gravitational waves", Journal of Instrumentation, Vol. 7, No. 03. (01 March 2012), P03012, doi:10.1088/1748-0221/7/03/p03012.

[7] R. Day, "A new FFT code: FOG Fast Fourier Transform Optical Simulation of Gravitational Wave Interferometers" - Talk at GWADW2012.

[8] G. Billingsley, "aLIGO ETM07 and ETM09 measurement for coating uniformity verification", LIGO technical note LIGO-T1300184-v1, https://dcc.ligo.org/LIGO-T1300184-v1

[9] J. Marque, A. Chiummo, and R. Day, "AdV - Stray Light Control: Impact of the coating ripples on the cryotrap baffles", Virgo technical note, VIR-0137A-13 https://tds.ego-gw.it/ql/?c=9483

[10] John C. Stover, "Optical Scattering: Measurement and Analysis", SPIE Press Monograph 1995

[11] C.Bradaschia, A.Pasqualetti, D.Sentenac, "Temperature effects on baffles and valves installed near cryotraps", Virgo technical note VIR-0132A-13, https://tds.ego-gw.it/ql/?c=9477

[12] Entegris UltraC Diamond coating specifications http://www.entegris.com/resources/assets/6102-7183-0512.pdf 3, 7

5

[13] Jean-Yves Vinet, "Backscattering noise from cryotraps", Virgo technical note VIR-0344A-10, https://tds.ego-gw.it/ql/?c=7498 5

5

5, 6

7

9

9

14